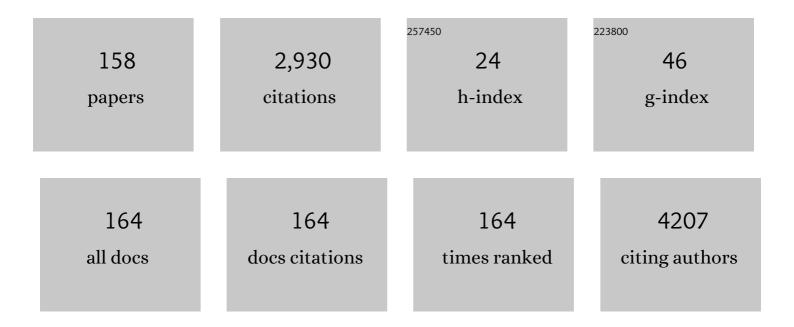
Enrico Grisan

List of Publications by Year in descending order

Source: https://exaly.com/author-pdf/5920317/publications.pdf Version: 2024-02-01



#	Article	IF	CITATIONS
1	epg5 knockout leads to the impairment of reproductive success and courtship behaviour in a zebrafish model of autophagy-related diseases. Biomedical Journal, 2022, 45, 377-386.	3.1	4
2	The primary visual cortex of Cetartiodactyls: organization, cytoarchitectonics and comparison with perissodactyls and primates. Brain Structure and Function, 2022, 227, 1195-1225.	2.3	13
3	OP16 The first virtual chromoendoscopy artificial intelligence system to detect endoscopic and histologic remission in Ulcerative Colitis. Journal of Crohn's and Colitis, 2022, 16, i017-i018.	1.3	1
4	OP15 A new simplified histology artificial intelligence system for accurate assessment of remission in Ulcerative Colitis. Journal of Crohn's and Colitis, 2022, 16, i015-i017.	1.3	5
5	An adaptive registration algorithm for zebrafish larval brain images. Computer Methods and Programs in Biomedicine, 2022, 216, 106658.	4.7	0
6	PICaSSO Histologic Remission Index (PHRI) in ulcerative colitis: development of a novel simplified histological score for monitoring mucosal healing and predicting clinical outcomes and its applicability in an artificial intelligence system. Gut, 2022, 71, 889-898.	12.1	45
7	Zebrafish Mutant Lines Reveal the Interplay between nr3c1 and nr3c2 in the GC-Dependent Regulation of Gene Transcription. International Journal of Molecular Sciences, 2022, 23, 2678.	4.1	8
8	Predicting functional impairment trajectories in amyotrophic lateral sclerosis: a probabilistic, multifactorial model of disease progression. Journal of Neurology, 2022, 269, 3858-3878.	3.6	7
9	A VIRTUAL CHROMOENDOSCOPY ARTIFICIAL INTELLIGENCE SYSTEM TO DETECT ENDOSCOPIC AND HISTOLOGIC REMISSION IN ULCERATIVE COLITIS. Endoscopy, 2022, 54, .	1.8	Ο
10	Constrained multiple instance learning for ulcerative colitis prediction using histological images. Computer Methods and Programs in Biomedicine, 2022, 224, 107012.	4.7	7
11	Deep learning for the prediction of treatment response in depression. Journal of Affective Disorders, 2021, 281, 618-622.	4.1	41
12	The claustrum of the sheep and its connections to the visual cortex. Journal of Anatomy, 2021, 238, 1-12.	1.5	7
13	Efficient clofilium tosylate-mediated rescue of POLG-related disease phenotypes in zebrafish. Cell Death and Disease, 2021, 12, 100.	6.3	13
14	Response to Biologics in Ibd Patients Assessed by Computerized Image Analysis of Probe Based Confocal Laser Endomicroscopy With Molecular Labeling. Endoscopy, 2021, 53, .	1.8	0
15	Deep-Learning Estimation of Perfusion Kinetic Parameters in Contrast-Enhanced Ultrasound Imaging. , 2021, , .		0
16	OP10 Response to biologics in IBD patients assessed by Computerized image analysis of Probe Based Confocal Laser Endomicroscopy with molecular labeling and gene expression profiling. Journal of Crohn's and Colitis, 2021, 15, S009-S010.	1.3	1
17	ID: 3523733 RESPONSE TO BIOLOGICS IN IBD PATIENTS ASSESSED BY COMPUTERIZED IMAGE ANALYSIS OF PROBE BASED CONFOCAL LASER ENDOMICROSCOPY WITH MOLECULAR LABELING. Gastrointestinal Endoscopy, 2021, 93, AB193.	1.0	0
18	Y705 and S727 are required for the mitochondrial import and transcriptional activities of STAT3, and for regulation of stem cell proliferation. Development (Cambridge), 2021, 148, .	2.5	38

#	Article	IF	CITATIONS
19	LPHN2 inhibits vascular permeability by differential control of endothelial cell adhesion. Journal of Cell Biology, 2021, 220, .	5.2	15
20	STW 5 Herbal Preparation Modulates Wnt3a and Claudin 1 Gene Expression in Zebrafish IBS-like Model. Pharmaceuticals, 2021, 14, 1234.	3.8	0
21	Real-time diameter of the fetal aorta from ultrasound. Neural Computing and Applications, 2020, 32, 6735-6744.	5.6	1
22	Multi-aspect testing and ranking inference to quantify dimorphism in the cytoarchitecture of cerebellum of male, female and intersex individuals: a model applied to bovine brains. Brain Structure and Function, 2020, 225, 2669-2688.	2.3	7
23	Single- and Multi-Distribution Dimensionality Reduction Approaches for a Better Data Structure Capturing. IEEE Access, 2020, 8, 207141-207155.	4.2	4
24	ls machine learning prediction of Aβ positivity consistent? An assessment of multiple datasets. Alzheimer's and Dementia, 2020, 16, e040990.	0.8	0
25	An Assay System to Evaluate Riboflavin/UV-A Corneal Phototherapy Efficacy in a Porcine Corneal Organ Culture Model. Animals, 2020, 10, 730.	2.3	5
26	miR-7 Controls the Dopaminergic/Oligodendroglial Fate through Wnt/β-catenin Signaling Regulation. Cells, 2020, 9, 711.	4.1	18
27	An objective comparison of detection and segmentation algorithms for artefacts in clinical endoscopy. Scientific Reports, 2020, 10, 2748.	3.3	41
28	Detecting and Characterizing the Fabella with High Frame-Rate Ultrasound Imaging. , 2020, , .		0
29	Feeding Entrainment of the Zebrafish Circadian Clock Is Regulated by the Glucocorticoid Receptor. Cells, 2019, 8, 1342.	4.1	21
30	Building A Reduced Dictionary Of Relevant Perfusion Patterns From Ceus Data For The Classification Of Testis Lesions. , 2019, , .		1
31	Does Quantification of Carotid Plaque Surface Irregularities Better Detect Symptomatic Plaques Compared to the Subjective Classification?. Journal of Ultrasound in Medicine, 2019, 38, 3163-3171.	1.7	5
32	The motor cortex of the sheep: laminar organization, projections and diffusion tensor imaging of the intracranial pyramidal and extrapyramidal tracts. Brain Structure and Function, 2019, 224, 1933-1946.	2.3	22
33	An Ultrasonographic Multiparametric Carotid Plaque Risk Index Associated with Cerebrovascular Symptomatology: A Study Comparing Color Doppler Imaging and Contrast-Enhanced Ultrasonography. American Journal of Neuroradiology, 2019, 40, 1022-1028.	2.4	9
34	The zebrafish orthologue of the human hepatocerebral disease gene <i>MPV17</i> plays pleiotropic roles in mitochondria. DMM Disease Models and Mechanisms, 2019, 12, .	2.4	21
35	The epg5 knockout zebrafish line: a model to study Vici syndrome. Autophagy, 2019, 15, 1438-1454.	9.1	16
36	Sparse Image Reconstruction for Contrast Enhanced Cardiac Ultrasound using Diverging Waves. ,		0

⁶ 2019, , .

#	Article	IF	CITATIONS
37	Super-Resolution Ultrasound Image Filtering with Machine-Learning to Reduce the Localization Error. , 2019, , .		4
38	Fetal Abdominal Aorta: Doppler and Structural Evaluation of Endothelial Function in Intrauterine Growth Restriction and Controls. Ultraschall in Der Medizin, 2019, 40, 55-63.	1.5	19
39	Prediction of Adverse Glycemic Events From Continuous Glucose Monitoring Signal. IEEE Journal of Biomedical and Health Informatics, 2019, 23, 650-659.	6.3	52
40	In-vivo Barrett's esophagus digital pathology stage classification through feature enhancement of confocal laser endomicroscopy. Journal of Medical Imaging, 2019, 6, 1.	1.5	9
41	Laminar Organization and Projections of the Motor Cortex of the Sheep. FASEB Journal, 2019, 33, 768.5.	0.5	Ο
42	Loss of cardiac Wnt/l²-catenin signalling in desmoplakin-deficient AC8 zebrafish models is rescuable by genetic and pharmacological intervention. Cardiovascular Research, 2018, 114, 1082-1097.	3.8	39
43	Fetal Abdominal Aorta: Doppler and Structural Evaluation of Endothelial Function in Intrauterine Growth Restriction and Controls. Ultraschall in Der Medizin, 2018, , .	1.5	1
44	Resolving single cells in heavily clustered Nissl-stained images for the analysis of brain cytoarchitecture. , 2018, , .		7
45	Temporal Convolution Networks for Real-Time Abdominal Fetal Aorta Analysis with Ultrasound. Lecture Notes in Computer Science, 2018, , 148-157.	1.3	0
46	Superpixel-based classification of gastric chromoendoscopy images. Proceedings of SPIE, 2017, , .	0.8	2
47	Grade and location of power Doppler are predictive of damage progression in rheumatoid arthritis patients in clinical remission by anti-tumour necrosis factor 1±. Rheumatology, 2017, 56, 1320-1325.	1.9	13
48	Boosted learned kernels for data-driven vesselness measure. , 2017, , .		0
49	Improving the quantification of contrast enhanced ultrasound using a Bayesian approach. Proceedings of SPIE, 2017, , .	0.8	0
50	Boosting the Battery Life of Wearables for Health Monitoring Through the Compression of Biosignals. IEEE Internet of Things Journal, 2017, 4, 1647-1662.	8.7	67
51	Bayesian Quantification of Contrast-Enhanced Ultrasound Images With Adaptive Inclusion of an Irreversible Component. IEEE Transactions on Medical Imaging, 2017, 36, 1027-1036.	8.9	7
52	Quantitative imaging by pixel-based contrast-enhanced ultrasound reveals a linear relationship between synovial vascular perfusion and the recruitment of pathogenic IL-17A-F+IL-23+ CD161+ CD4+ T helper cells in psoriatic arthritis joints. Clinical Rheumatology, 2017, 36, 391-399.	2.2	21
53	Glucocorticoids promote Von Hippel Lindau degradation and Hif-1α stabilization. Proceedings of the National Academy of Sciences of the United States of America, 2017, 114, 9948-9953.	7.1	49
54	A possible new approach in the prediction of late gestational hypertension. Medicine (United States), 2017, 96, e5515.	1.0	10

#	Article	lF	CITATIONS
55	Cortical Thickness variability in Multiple Sclerosis: The role of lesion segmentation and filling. , 2017, , .		0
56	From macro to nano: Linking quantitative CEUS perfusion parameters to CD4+ T cells subtypes in spondyloarthtitis. , 2017, , .		0
57	Detection of a slow-flow component in contrast-enhanced ultrasound of the synovia for the differential diagnosis of arthritis. Proceedings of SPIE, 2017, , .	0.8	Ο
58	Tcf7l2 plays pleiotropic roles in the control of glucose homeostasis, pancreas morphology, vascularization and regeneration. Scientific Reports, 2017, 7, 9605.	3.3	16
59	A novel non-rigid registration algorithm for zebrafish larval images. , 2017, 2017, 321-324.		Ο
60	Growth Abnormalities of Fetuses and Infants. BioMed Research International, 2017, 2017, 1-4.	1.9	5
61	Treponema pallidum (syphilis) antigen TpF1 induces angiogenesis through the activation of the IL-8 pathway. Scientific Reports, 2016, 6, 18785.	3.3	27
62	Automatic classification of small bowel mucosa alterations in celiac disease for confocal laser endomicroscopy. Proceedings of SPIE, 2016, , .	0.8	0
63	Monitoring Wnt Signaling in Zebrafish Using Fluorescent Biosensors. Methods in Molecular Biology, 2016, 1481, 81-94.	0.9	19
64	Down-regulation of coasy, the gene associated with NBIA-VI, reduces Bmp signaling, perturbs dorso-ventral patterning and alters neuronal development in zebrafish. Scientific Reports, 2016, 6, 37660.	3.3	42
65	Biomedical signal compression with time- and subject-adaptive dictionary for wearable devices. , 2016, , .		13
66	FRI0065â€Presence, Grade and Location of Power Doppler Predict Progression of Radiographic Damage in TNFα Blocker Induced Clinical Remission in Rheumatoid Arthritis Patients. Annals of the Rheumatic Diseases, 2016, 75, 449.2-449.	0.9	0
67	Superpixel-based automatic segmentation of villi in confocal endomicroscopy. , 2016, , .		2
68	Automatic classification of endoscopic images for premalignant conditions of the esophagus. , 2016, , .		4
69	A novel approach to aortic intima-media thickness quantification from fetal ultrasound images. , 2015, , .		Ο
70	A fully automated approach to aortic distensibility quantification from fetal ultrasound images. , 2015, , .		0
71	Fully-automated identification and segmentation of aortic lumen from fetal ultrasound images. , 2015, 2015, 153-6.		5
72	A novel approach to motion correction for ASL images based on brain contours. , 2015, , .		0

#	Article	IF	CITATIONS
73	Quantification of kidneys from 3D ultrasound in pediatric hydronephrosis. , 2015, 2015, 157-60.		4
74	Pixel-based approach to assess contrast-enhanced ultrasound kinetics parameters for differential diagnosis of rheumatoid arthritis. Journal of Medical Imaging, 2015, 2, 034503.	1.5	15
75	Toward lightweight biometric signal processing for wearable devices. , 2015, 2015, 4190-3.		5
76	Detection and density estimation of goblet cells in confocal endoscopy for the evaluation of celiac disease. , 2015, 2015, 6248-51.		2
77	Semiautomatic detection of villi in confocal endoscopy for the evaluation of celiac disease. , 2015, 2015, 8143-6.		4
78	Effects of mud-bath therapy in psoriatic arthritis patients treated with TNF inhibitors. Clinical evaluation and assessment of synovial inflammation by contrast-enhanced ultrasound (CEUS). Joint Bone Spine, 2015, 82, 104-108.	1.6	38
79	Vascular perfusion kinetics by contrast-enhanced ultrasound are related to synovial microvascularity in the joints of psoriatic arthritis. Clinical Rheumatology, 2015, 34, 1903-1912.	2.2	36
80	A supervised learning approach for the robust detection of heart beat in plethysmographic data. , 2015, 2015, 5825-8.		16
81	Polarization Sensitive Optical Coherence Tomography for Zebrafish Imaging. , 2015, , .		ο
82	Corneal confocal microscopy reveals trigeminal small sensory fiber neuropathy in amyotrophic lateral sclerosis. Frontiers in Aging Neuroscience, 2014, 6, 278.	3.4	66
83	Dynamic automated synovial imaging (DASI) for differential diagnosis of rheumatoid arthritis. , 2014, , .		2
84	A comparison of region-based and pixel-based CEUS kinetics parameters in the assessment of arthritis. , 2014, , .		3
85	Analytic heuristics for a fast DSC-MRI. Proceedings of SPIE, 2014, , .	0.8	0
86	A Smad3 transgenic reporter reveals TGF-beta control of zebrafish spinal cord development. Developmental Biology, 2014, 396, 81-93.	2.0	52
87	A boosted optimal linear learner for retinal vessel segmentation. , 2014, , .		Ο
88	Estimation of prenatal aorta intima-media thickness from ultrasound examination. Physics in Medicine and Biology, 2014, 59, 6355-6371.	3.0	14
89	MR and CEUS monitoring of patients with severe rheumatoid arthritis treated with biological agents: a preliminary study. Radiologia Medica, 2014, 119, 422-431.	7.7	10
90	Baseline constrained reconstruction of DSC-MRI tracer kinetics from sparse fourier data. , 2014, , .		0

6

#	Article	IF	CITATIONS
91	Computer-assisted automated image recognition of celiac disease using confocal endomicroscopy. , 2014, , .		2
92	Early origins of adult disease: Low birth weight and vascular remodeling. Atherosclerosis, 2014, 237, 391-399.	0.8	153
93	AB0953â€A Comparison of Region-Based and Pixel-Based CEUS Kinetics Parameters in the Differentiation of Rheumatoid Arthritis and Simil-Rheumatoid Psoriatic Arthritis. Annals of the Rheumatic Diseases, 2014, 73, 1115.2-1115.	0.9	0
94	SAT0175â€Dynamic Automated Synovial Imaging (DASI) for Differentiating between Rheumatoid Arthritis and Simil-Rheumatoid Psoriatic Arthritis. Annals of the Rheumatic Diseases, 2014, 73, 653.3-654.	0.9	0
95	Automated Estimation of Aortic Intima-Media Thickness from Fetal Ultrasound. Lecture Notes in Computer Science, 2014, , 33-40.	1.3	2
96	Stacked Models for Efficient Annotation of Brain Tissues in MR Volumes. IFMBE Proceedings, 2014, , 261-264.	0.3	0
97	Quantitative Assessment of Prenatal AorticWall Thickness in Gestational Diabetes. IFMBE Proceedings, 2014, , 249-252.	0.3	Ο
98	Learning Optimal Matched Filters for Retinal Vessel Segmentation with ADA-Boost. IFMBE Proceedings, 2014, , 380-383.	0.3	0
99	Reconstruction of DSC-MRI Data from Sparse Data Exploiting Temporal Redundancy and Contrast Localization. IFMBE Proceedings, 2014, , 225-228.	0.3	1
100	Data-Driven Learning to Detect Characteristic Kinetics in Ultrasound Images of Arthritis. Lecture Notes in Computer Science, 2014, , 17-24.	1.3	2
101	Semiautomatic Evaluation of Crypt Architecture and Vessel Morphology in Confocal Microendoscopy: Application to Ulcerative Colitis. IFMBE Proceedings, 2014, , 435-438.	0.3	1
102	Improved detection of synovial boundaries in ultrasound examination by using a cascade of active-contours. Medical Engineering and Physics, 2013, 35, 188-194.	1.7	18
103	Contrast-enhanced ultrasound findings in soft-tissue lesions: preliminary results. Journal of Ultrasound, 2013, 16, 21-27.	1.3	13
104	Hybrid patch-based and image-wide classification of confocal laser endomicroscopy images in Barrett's esophagus surveillance. , 2013, , .		7
105	Spline-based refinement of vessel contours in fundus retinal images for width estimation. , 2013, , .		6
106	A radiographic-based method for marginal bone loss measurement in dental implants. , 2013, , .		1
107	FRI0478â€Dynamic automated synovial imaging (DASI) For differentiating between rheumatoid arthritis and other forms of arthritis: automated versus manual interpretation in contrast-enhanced ultrasound. Annals of the Rheumatic Diseases, 2013, 72, A536.3-A537.	0.9	2
108	FRI0477â€Validity of contrast-enhanced ultrasound (CEUS) in the detection of synovial inflammation in rheumatoid arthritis compared to power doppler in contrast-enhanced mri controlled pilot study. Annals of the Rheumatic Diseases, 2013, 72, A536.2-A536.	0.9	1

#	Article	IF	CITATIONS
109	AB0716â€Update of disease activity assessment in rheumatoid arthritis: comparison between clinical, ultrasound and mri scores and introduction of volumetric inflammation measure concept. Annals of the Rheumatic Diseases, 2013, 72, A1006.3-A1006.	0.9	0
110	Developmental Programming of Cardiovascular Risk in Intrauterine Growth-Restricted Twin Fetuses According to Aortic Intima Thickness. Journal of Ultrasound in Medicine, 2013, 32, 279-284.	1.7	22
111	Automatic Analysis of Pediatric Renal Ultrasound Using Shape, Anatomical and Image Acquisition Priors. Lecture Notes in Computer Science, 2013, 16, 259-266.	1.3	11
112	Stability of a telerobotic manipulation system with proximity—Based haptic feedback. , 2012, , .		1
113	A telerobotic manipulation system for an immerse ultrasonic examination using haptic constraints. , 2012, , .		3
114	Supervised classification of brain tissues through local multi-scale texture analysis by coupling DIR and FLAIR MR sequences. , 2012, , .		3
115	Estimation of prenatal aorta intima-media thickness in ultrasound examination. Proceedings of SPIE, 2012, , .	0.8	0
116	A review of thresholding strategies applied to human chromosome segmentation. Computer Methods and Programs in Biomedicine, 2012, 108, 679-688.	4.7	47
117	P.10.1 COMPUTER AIDED DIAGNOSIS OF BARRETT'S ESOPHAGUS USING CONFOCAL LASER ENDOMICROSCOPY: PRELIMINARY DATA. Digestive and Liver Disease, 2012, 44, S147-S148.	0.9	3
118	239 Computer Aided Diagnosis of Barrett's Esophagus Using Confocal Laser Endomicroscopy: Preliminary Data. Gastrointestinal Endoscopy, 2012, 75, AB126.	1.0	8
119	Image-level tortuosity estimation in wide-field retinal images from infants with Retinopathy of Prematurity. , 2012, 2012, 4958-61.		13
120	A modular framework for the automatic classification of chromosomes in Q-band images. Computer Methods and Programs in Biomedicine, 2012, 105, 120-130.	4.7	27
121	Textureless Macula Swelling Detection With Multiple Retinal Fundus Images. IEEE Transactions on Biomedical Engineering, 2011, 58, 795-799.	4.2	38
122	Automatic vessel segmentation in wide-field retina images of infants with Retinopathy of Prematurity. , 2011, 2011, 3954-7.		10
123	An improved classification scheme for chromosomes with missing data. , 2011, 2011, 5072-5.		6
124	Semi Automatic Detection of Synovial Boundaries in Water-Immersion Ultrasound Examination. , 2011, , \cdot		0
125	Unsupervised Segmentation of Brain Tissues using Multiphase Level Sets on Multiple MRI Sequences. , 2011, , .		0
126	Automatic Segmentation and Disentangling of Chromosomes in Q-Band Prometaphase Images. IEEE Transactions on Information Technology in Biomedicine, 2009, 13, 575-581.	3.2	60

#	Article	IF	CITATIONS
127	A Markov Random Field Approach to Outline Lesions in Fundus Images. IFMBE Proceedings, 2009, , 472-475.	0.3	4
128	Dynamic Time Warping and Cross Correlation for the estimation of cell movements in conjunctival capillaries: a comparison through simulation. IFMBE Proceedings, 2009, , 112-115.	0.3	1
129	Estimation of Real-Time Red Blood Cell Velocity in Conjunctival Vessels using a Modified Dynamic-Time-Warping Approach. IFMBE Proceedings, 2009, , 480-483.	0.3	2
130	Retinal Vessel Axis Estimation through a Multi-Directional Graph Search Approach. IFMBE Proceedings, 2009, , 137-140.	0.3	5
131	A Novel Method for the Automatic Grading of Retinal Vessel Tortuosity. IEEE Transactions on Medical Imaging, 2008, 27, 310-319.	8.9	192
132	Automatic Recognition of Corneal Nerve Structures in Images from Confocal Microscopy. , 2008, 49, 4801.		87
133	An improved system for the automatic estimation of the Arteriolar-to-Venular diameter Ratio (AVR) in retinal images. , 2008, 2008, 3550-3.		26
134	Automatic classification of chromosomes in Q-band images. , 2008, 2008, 1911-4.		29
135	An automatic system for the estimation of generalized arteriolar narrowing in retinal images. Annual International Conference of the IEEE Engineering in Medicine and Biology Society, 2007, 2007, 6464-7.	0.5	23
136	Boosting Invariance and Efficiency in Supervised Learning. , 2007, , .		7
137	A new computerized method for the assessment of skin lesions in localized scleroderma. Rheumatology, 2007, 46, 856-860.	1.9	65
138	3-D Retinal Surface Inference: Stereo or Monocular Fundus Camera?. Annual International Conference of the IEEE Engineering in Medicine and Biology Society, 2007, 2007, 896-9.	0.5	4
139	Automatic segmentation of chromosomes in Q-band images. Annual International Conference of the IEEE Engineering in Medicine and Biology Society, 2007, 2007, 5513-6.	0.5	14
140	Evaluation of repeatability for the automatic estimation of endothelial cell density in donor corneas. British Journal of Ophthalmology, 2007, 91, 1213-1215.	3.9	9
141	No wavefront sensor adaptive optics system for compensation of primary aberrations by software analysis of a point source image 2 Tests. Applied Optics, 2007, 46, 6427.	2.1	3
142	No wavefront sensor adaptive optics system for compensation of primary aberrations by software analysis of a point source image 1 Methods. Applied Optics, 2007, 46, 6434.	2.1	10
143	Segmentation of candidate dark lesions in fundus images based on local thresholding and pixel density. Annual International Conference of the IEEE Engineering in Medicine and Biology Society, 2007, 2007, 6736-9.	0.5	27
144	Analysis of corneal images for the recognition of nerve structures. , 2006, 2006, 4739-42.		18

#	Article	IF	CITATIONS
145	Detecting false vessel recognitions in retinal fundus analysis. , 2006, 2006, 4449-52.		1
146	Defocus Inpainting. Lecture Notes in Computer Science, 2006, , 349-359.	1.3	4
147	Detecting false vessel recognitions in retinal fundus analysis. Annual International Conference of the IEEE Engineering in Medicine and Biology Society, 2006, , .	0.5	Ο
148	Luminosity and contrast normalization in retinal images. Medical Image Analysis, 2005, 9, 179-190.	11.6	262
149	Aberration estimation from single point image in a simulated adaptive optics system. , 2005, 2005, 3173-6.		0
150	A lattice estimation approach for the automatic evaluation of corneal endothelium density. , 2005, 2005, 1700-3.		6
151	A new system for the automatic estimation of endothelial cell density in donor corneas. British Journal of Ophthalmology, 2005, 89, 306-311.	3.9	39
152	Detection of Optic Disc in Retinal Images by Means of a Geometrical Model of Vessel Structure. IEEE Transactions on Medical Imaging, 2004, 23, 1189-1195.	8.9	371
153	A new tracking system for the robust extraction of retinal vessel structure. , 2004, 2004, 1620-3.		42
154	Detecting the optic disc in retinal images by means of a geometrical model of vessel network. , 0, , .		2
155	A divide et impera strategy for automatic classification of retinal vessels into arteries and veins. , 0, , .		84
156	A novel method for the automatic evaluation of retinal vessel tortuosity. , 0, , .		19
157	Model-Based Illumination Correction in Retinal Images. , 0, , .		18
158	Quantitative ultrasound for diagnosis and assessment of rheumatoid arthritis. SPIE Newsroom, 0, , .	0.1	4